Available online at www.sciencedirect.com
ScienceDirect
Journal of Sound and Vibration 313 (2008) 617–630
JOURNAL OF SOUND AND VIBRATION
www.elsevier.com/locate/jsvi

An analytical, numerical, and experimental study of the axisymmetric vibrations of a short cylinder

Francisco J. Nieves[a,*], Francisco Gascón[a], Ana Bayón[b]

[a]*Departamento de Física Aplicada II, Universidad de Sevilla, ETS de Arquitectura, Avd. Reina Mercedes, 2, 41012 Sevilla, Spain*
[b]*Departamento de Física Aplicada a los Recursos Naturales, Universidad Politécnica de Madrid, ETSI Minas, c/ Ríos Rosas, 21, 28003 Madrid, Spain*

Received 27 July 2007; received in revised form 14 November 2007; accepted 21 November 2007
Handling Editor: A.V. Metrikine
Available online 29 January 2008

Abstract

This paper presents a study of standing axisymmetric waves in homogeneous, isotropic, linear, and elastic cylinders whose length and diameter are of the same order of magnitude. It is analytically demonstrated that only materials with a Poisson's ratio equal to zero can vibrate in pure radial and longitudinal axisymmetric modes and, hence, the universal frequencies, independent of Poisson's ratio, and the corresponding universal aspect ratios can be accurately calculated. The Ritz method is applied to numerically determine the natural frequencies and the mode shapes of finite cylinders. Vibration of a cylinder in the neighbourhood of the universal point is analysed. Both free and forced vibrations are experimentally detected by using a laser speckle interferometer that allows the determination of the natural frequencies and the mode shapes. From the numerical calculations, it is confirmed that, for materials with Poisson's ratio not equal to zero, no crossings occur between the curves of non-dimensional frequency versus aspect ratio, neither for antisymmetric modes themselves nor for symmetric modes. There is a good agreement between the analytical solutions, the numerical results, and the experimental measurements.

1. Introduction

The study of propagation of waves in cylinders on the basis of the classical theory of elasticity is well known [1]. The Pochhamer-Chree solution is exact for an infinitely long isotropic cylinder that is stress free at the cylindrical surface. For finite-length cylinders with free ends, there are no analytical solutions to the equations of motion that fulfil the requirements so that the shear and traction stresses at both ends vanish.

The non-dimensional frequency $\Omega = \pi f D\sqrt{\rho/G}$ is often used for the sake of simplicity, where f is the ordinary frequency, measured in Hertz, D the diameter of the rod, ρ the density, and G the shear modulus. An analytical study of the propagation of axisymmetric waves in a cylinder shows [2] that the shear stress identically equals zero at all points of the cylinder for an infinite set of values of Ω. Such values are those for

*Corresponding author.
E-mail address: nieves@us.es (F.J. Nieves).

0022-460X/$ - see front matter © 2007 Elsevier Ltd. All rights reserved.
doi:10.1016/j.jsv.2007.11.041

which the Bessel function of the first kind and order one, $J_1(kD/2)$, is a maximum or a minimum, where k is the wavenumber. The maxima and minima found in the scientific literature occur for $\sqrt{2}kD/2 = 2.6036, 7.5392, \ldots$. The significance of these maxima or minima is that, at these frequencies, a finite-length rod will be an integer number of half-wavelengths long. These points are universal in the sense that they are independent of Poisson's ratio. For frequencies other than universal frequencies, the condition that the cylinder length is an integer number of half-wavelengths is not satisfied.

Zemanek [2] found an approximate solution for symmetric wave propagation in a semi-infinite cylinder by assuming that one reflected wave and other waves with complex propagation constants are generated at the traction-free surface. A similar technique has also been recently applied to a finite cylinder with various end conditions and the wave guide model proposed provides accurate results [3]. Hutchinson [4–7] developed a solution of the general three-dimensional elasticity for vibrations of finite cylinders. His three-dimensional solution is based on combining exact solutions of the governing equations in series, which satisfy term by term some of the boundary conditions exactly; the remaining boundary conditions are satisfied by orthogonalization on the boundaries. Comparison of Hutchinson's solution [8,9] with that obtained by the Ritz method for vibrating finite cylinders demonstrates the high accuracy that can be achieved with his series solution. Lusher and Hardy [10] extended Hutchinson's method for transversely isotropic cylinders.

Many studies are found in the scientific literature that use numerical methods to determine the vibration modes of finite-length cylinders. One widely used procedure is the Ritz method. The procedure of Rumermann and Raynor [11] involves representation of the components of displacement in series of the corresponding pure radial and axial modes of the infinite cylinder. Senoo et al. [12] use Legendre polynomials along the cylinder axis as basis functions to calculate the elastic constants. Heyliger [13] used power series in the coordinate directions as the approximating functions to find estimates for the axisymmetric free vibrations of finite cylinders composed of an isotropic material or a material with hexagonal symmetry. Visscher et al. [14] proposed a powerful approach for the general solution of the weak form of the equations of motion formulated in rectangular Cartesian coordinates. In later work, Heyliger and Jilani [15] used the Ritz method to extend previous analysis to include the complete vibrations of a solid isotropic cylinder and to study the free vibration of hollow and orthotropic cylinders of finite length. The study by Heyliger and Johnson [16] provides the results for resonant frequencies of finite elastic cylinders with trigonal material symmetry. The problem is considered in both rectangular coordinates and cylindrical coordinates. One notable study is that by Leissa and So [17] who apply the Ritz method in a straightforward, uncomplicated manner to the study of vibrations of isotropic cylinders of finite length that have arbitrary boundary conditions; algebraic polynomials of the cylindrical coordinates are used to represent the displacements. Different combinations of increasing exponents are tested in order to determine the lowest frequency for a mode with the smallest determinant size. The convergence scheme is followed in a table.

In this work, the Ritz method is used as proposed by Leissa and So [17] to calculate natural frequencies and mode shapes for axisymmetric vibrations of isotropic finite cylinders. It differs from their approach in the procedure followed to determine the optimum upper limits of the exponents of the series used as displacement functions. In this paper, the Ritz method is optimally applied by following an automatic iterative process described in Ref. [18] that provides the best combination of exponents for a determinant size. No tables are needed to compare the results in order to seek the best solution.

Moreover, an analytical study of radial and longitudinal vibrations of short cylinders is presented. The purpose is to analytically determine accurate values for the universal frequencies, to prove that both vibration modes are possible only if Poisson's ratio is zero, and to find the existence of multiple frequencies in that case.

An analysis of the mode shapes in the neighbourhood of the first universal point is also included. Special attention is paid to the crossings of the curves for the different modes in the plot of frequency versus slenderness. The aforesaid optimization procedure is used in Section 6 in the analysis of the apparent frequency crossing points. In addition, this study seeks to set out some results according to not only the value of the frequency but also the form of the mode shape. The analytical, numerical, and experimental results are in good agreement.

2. Study of pure radial and pure longitudinal modes—analytical solutions

This study is focussed only on the analysis of axisymmetric vibrations of linear elastic cylinders, except torsional waves. Hence, displacements radial u and longitudinal w are independent of coordinate θ and the tangential component v is zero. Hooke's law gives the following for the stress tensor:

$$\begin{aligned} p_{rr} &= \lambda\left(\frac{u}{r}+\frac{\partial u}{\partial r}+\frac{\partial w}{\partial z}\right)+2G\frac{\partial u}{\partial r},\\ p_{r\theta} &= 0,\\ p_{rz} &= G\left(\frac{\partial u}{\partial z}+\frac{\partial w}{\partial r}\right),\\ p_{\theta\theta} &= \lambda\left(\frac{u}{r}+\frac{\partial u}{\partial r}+\frac{\partial w}{\partial z}\right)+2G\frac{u}{r},\\ p_{\theta z} &= 0,\\ p_{zz} &= \lambda\left(\frac{u}{r}+\frac{\partial u}{\partial r}+\frac{\partial w}{\partial z}\right)+2G\frac{\partial w}{\partial z}, \end{aligned} \tag{1}$$

where λ is the Lamé constant. The momentum equations expressed in terms of displacements are for a continuous medium free from body forces:

$$\begin{aligned} \frac{\partial p_{rr}}{\partial r}+\frac{\partial p_{rz}}{\partial z}+\frac{p_{rr}-p_{\theta\theta}}{r} &= \rho\frac{\partial^2 u}{\partial t^2},\\ \frac{\partial p_{rz}}{\partial r}+\frac{\partial p_{zz}}{\partial z}+\frac{p_{rz}}{r} &= \rho\frac{\partial^2 w}{\partial t^2}. \end{aligned} \tag{2}$$

2.1. Standing radial vibration of cylinders

Let us study the possibility of the existence of a standing wave in a cylinder in which the particle displacement is entirely radial, i.e., $u = U(r)\exp(\mathrm{i}\omega t)$, $w = 0$.

Substitution of the proposed displacement in Eqs. (1) and then in Eqs. (2) gives the only one non-trivial equation whose solution is given by

$$U = CJ_1(kr), \tag{3}$$

where the wavenumber is $k = \omega/(\sqrt{(\lambda+2G)/\rho})$.

On application of the boundary condition that the cylindrical surface is traction-free, $p_{rr} = 0$ at $r = D/2$, the first of Eq. (1) yields

$$2(\lambda+G)J_1(kD/2) = (\lambda+2G)(kD/2)J_2(kD/2), \tag{4}$$

where J_2 is the Bessel function of the first kind and order 2. This equation gives the infinite values of k and, hence, of ω for all possible radial vibrations of infinitely long cylinders. Substitution of λ and G, as functions of Young's modulus E and Poisson ratio $v\lambda = Ev/[(1+v)(1-2v)]$ and $G = E/[2(1+\mathrm{v})]$, into Eq. (4), and taking into account the expression of J_2 in terms of J_1 and J_0 [19], yields the following equation:

$$(1-2v)J_1(kD/2) = (1-v)(kD/2)J_0(kD/2). \tag{5}$$

If the origin of coordinates is chosen at the centre of a finite-length cylinder with length L, its flat ends are located at $z = \pm L/2$. In addition to the condition at the cylindrical surface, the boundary condition at the traction-free ends must also be satisfied, $p_{zz}|_{z=\pm L/2} = 0$, and the latter can be satisfied only if

$$\lambda\left(\frac{\mathrm{d}U}{\mathrm{d}r}+\frac{U}{r}\right) = 0. \tag{6}$$

If the material has a Poisson's ratio $v \neq 0$ (and $0 < v < 0.5$), then the Lamé constant $\lambda \neq 0$ and Eq. (6) implies $dU/dr + U/r = 0$, whose solution is $U = c/r$. This result is impossible since the amplitude along the axis must be zero. Therefore, it can be concluded that pure radial vibrations cannot occur in a finite cylinder with a Poisson's ratio other than zero.

If $v = 0$, it is obvious that pure radial vibrations can occur and the solution to Eq. (5) is obtained by numerical calculation using a computer program. The results found are

$$kD/2 = 1.841183785\ldots,\ 5.331442733\ldots,\ 8.536316367\ldots,\ \ldots\ .$$

Since in this case $\lambda = 0$, $k = \omega/(\sqrt{2G/\rho})$, then the non-dimensional frequencies for the radial vibrations obtained are equal to

$$\Omega = (\sqrt{2})kD/2 = 2.60382707\ldots,\ 7.53979861\ldots,\ 12.07217438\ldots,\ \ldots \quad \forall n = 0. \tag{7}$$

Taking four decimal figures in the results for Ω, the non-dimensional frequencies are $\Omega = 2.6038$, 7.5398, 12.0722, …. These values of Ω are similar to those given in the introduction when $J_1(kD/2)$ is a maximum or a minimum. This similarity is not a coincidence. In fact, if $J_1(x)$ is a maximum or a minimum, then its derivative is zero, and the aforesaid property of the Bessel functions leads to the equation $J_1(x) - xJ_0(x) = 0$, which takes the same form as the aforementioned Eq. (5) with $v = 0$. Hence, the non-dimensional frequencies for which shear stress equals zero at all points of a infinitely long cylinder should take the same values as those for the radial frequencies of a finite-length cylinder whose Poisson's ratio is zero. The difference between the values given by other authors [2] and those obtained here (7) is at least two units in the fifth significant figure. Such a difference may be mainly attributed to two factors: (1) the computers used were not accurate enough, and (2) the function $J_1(x)$ is very smooth in the neighbourhood of its maxima and minima, making the accurate determination of the value of x difficult. On the other hand, the function $J_1(x) - xJ_0(x)$ varies greatly on crossing the x-axis, which allows one to find the solution for x with great accuracy.

The values of Ω given by Eq. (7) for the pure radial vibration show that Ω is independent of L/D. On the plot of Ω versus L/D, the graph is a set of straight lines parallel to the L/D axis. The quotient of the length and diameter of a cylinder L/D is called the slenderness or aspect ratio.

The set of frequencies given by Eq. (7) is numerically equal to the so-called universal frequencies. Each universal frequency is associated with a universal slenderness ratio [20]. For the above-calculated values of the universal frequencies, the corresponding universal slenderness ratios are 0.8531, 0.8840, … . All of the curves Ω–L/D for the symmetric modes pass through these universal values regardless of Poisson's ratio. The pure radial symmetric modes studied also pass through the universal values of Ω, the corresponding straight lines being parallel to the L/D axis.

2.2. Standing longitudinal vibration of cylinders

Let us now study standing longitudinal axisymmetric vibrations in cylinders. Since longitudinal elongation of a material with a Poisson's ratio of zero does not induce a lateral motion, one of the possible mode shapes is that associated with a purely longitudinal motion, which is obviously characteristic of these materials with $v = 0$. Here, the condition $v = 0$ is proved to be a necessary condition.

A harmonic solution is first considered which has the form: $u = 0$, $w = W(z)\exp(i\omega t)$. Eqs. (1) and (2) reduce to a second-order differential equation. As p_{rr} is zero at the cylindrical surface, $\lambda[dW/dz]_{r=D/2} = 0$, it is found that the only non-trivial and finite motion is for $\lambda = 0$ which implies $v = 0$, therefore $G = E/2$, and the amplitude W is then given by

$$W = C\sin\left(\frac{\omega}{\sqrt{E/\rho}}z + \varphi\right) \quad \forall n = 0, \tag{8}$$

where the velocity corresponds to that of longitudinal waves propagating along a slender rod.

For a finite cylinder the boundary condition at the ends of the cylinder, $p_{zz} = 0$, should also be taken into account, which leads to the solution for ω:

$$\omega = \frac{N\pi}{L}\sqrt{\frac{E}{\rho}} \Rightarrow \Omega = \frac{N\pi}{\sqrt{2}L/D} \quad \forall \nu = 0. \tag{9}$$

This result coincides with that found using the elemental theory, as expected, since such a theory disregards the effect of the lateral contraction. A set of equilateral hyperbolas is obtained when drawing Ω versus L/D.

Let us now consider longitudinal displacements of the form $u = 0$, $w = W(r)\exp(i\omega t)$. Eqs. (1) and (2) reduce to the Bessel equation of the first kind and order zero, whose finite solution at $r = 0$ is

$$W = CJ_0\left(\sqrt{\frac{\rho\omega^2}{G}}r\right). \tag{10}$$

The boundary condition on the cylindrical surface is that the only non-zero component of the stress tensor, p_{rz}, be equal to zero at $r = D/2$, which leads to the approximate solutions

$$\Omega = 0, \quad 3.8317, \quad 7.0156, \quad \ldots. \tag{11}$$

For a finite cylinder a boundary condition at the cylinder's ends is $p_{rz} = 0$ at $z = \pm L/2$. Therefore, from Eqs. (1) and (10) it follows that $C = 0$ and there is no motion. It is then concluded that the solution proposed is not admissible for a finite cylinder.

The analysis performed in this section shows that a short cylinder can only undergo pure longitudinal axisymmetric vibrations provided that the amplitude depends on z and if and only if Poisson's ratio is zero. However, such a cylinder can vibrate axisymmetrically in its pure radial modes if the amplitude depends on r and if and only if its Poisson's ratio is zero.

2.3. Case of multiple frequencies. Degeneration

The results obtained in Eq. (7) for the non-dimensional frequencies in the case of pure radial vibrations of cylinders with Poisson's ratio equal to zero correspond to symmetric modes with respect to the plane $z = 0$. Furthermore, for pure longitudinal vibrations the frequencies are given by Eq. (9). Equating, for instance, the lowest longitudinal frequency, $N = 1$, which is symmetrical, with the lowest radial frequency, also symmetrical, it is found that $L/D = 0.85314$. For this value of slenderness the curves of Ω versus L/D cross at a point and hence the frequency corresponding to $\Omega = 2.6038$ is a multiple value for the symmetric modes, with a degree of multiplicity of at least two. The same results were obtained in a previous study [20] of the universal point and its neighbourhood using numerical calculations ($\Omega_u = 2.6036$ and $L/D = 0.85322$). It seems evident that for other universal frequencies, with their corresponding universal slenderness ratios, the results will be similar.

3. Numerical study of axisymmetric vibrations of a cylinder

3.1. Numerical calculation of frequencies and mode shapes

As aforesaid in Introduction, the Ritz method is applied to axisymmetric vibrations of finite cylinders with stress-free boundary conditions following the optimization procedure described in Ref. [18], which gives the square of the non-dimensional frequencies (Ω^2) and the coefficients of the polynomials. The convergence of the results is dependent on the maximum values of the exponents, the interval of values of L/D under consideration, and frequency Ω. The results of many calculations led us to infer the following empirical rule: for values of slenderness greater than the lowest universal slenderness ratio, the power of z should be larger than that of r as a result of the complexity of the modes along the OZ axis. However, For smaller values of such slenderness, the largest power corresponds to variable r. Therefore, it seems that at the first universal point, the significance of the length of the cylinder in its dynamic behaviour is the same as that of the diameter.

3.2. Numerical results

The numerical calculations allow one to carry out a wider study of the vibration of a cylinder than that presented in Section 2. In this section, two applications are reported. Other numerical calculations are described in Sections 5 and 6.

(1) The Ritz method is first applied to calculate the frequencies Ω corresponding to the lowest symmetric and antisymmetric modes for a material with $\nu = 0$. For each value of L/D, the modes are arranged according to the increasing value of the frequency. The results shown in Fig. 1 are for the symmetric modes. The curves in this figure are formed by segments connecting the points associated with the non-dimensional frequencies for the values of the slenderness from 0.05 to 3, the increment being 0.05 or less. The accuracy of the numerical calculations for Ω for each L/D has been estimated to be 10^{-6} for the lowest frequencies and 10^{-1} for the highest, by a convergence study that includes up to about a hundred of coefficients. The figure corresponding to antisymmetric modes is not shown here.
A first conclusion deduced from the numerical results shown in Fig. 1 is that for the pure radial and longitudinal modes the relationship between the non-dimensional frequency and the slenderness is the same as that found analytically. Note that the pure radial modes appear as horizontal straight lines passing through the universal frequencies, while the curves for the pure longitudinal modes appear as equilateral hyperbolas, where the product of Ω and L/D is an integer number of times $\pi/\sqrt{2}$, which together confirm the accuracy of the numerical calculations.
When analysing the crossings of the curves in the graph of Ω–L/D it should be clarified whether either curves for the lowest frequency, or curves for the same mode are taken into consideration. The curve for $s1$ refers to the lowest symmetric frequency. However, it seems more reasonable that curves corresponding to the same mode be plotted.

(2) Calculation of the mode shapes at the universal point for a Poisson's ratio equal to zero shows that in addition to the longitudinal and radial modes another possible symmetrical mode shape is that with circular vortices as it is shown in Section 5.

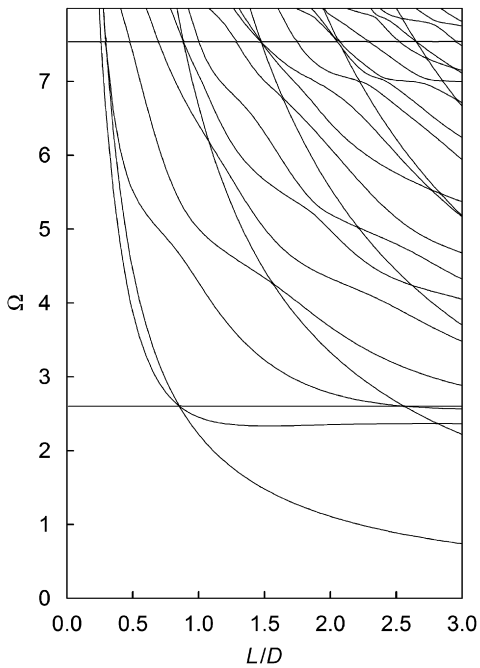

Fig. 1. The lowest non-dimensional frequencies versus slenderness for the axial symmetric vibration of a short cylinder with Poisson's ratio zero. Note the apparent crossing of the three curves corresponding to $s1$, $s2$, and $s3$.

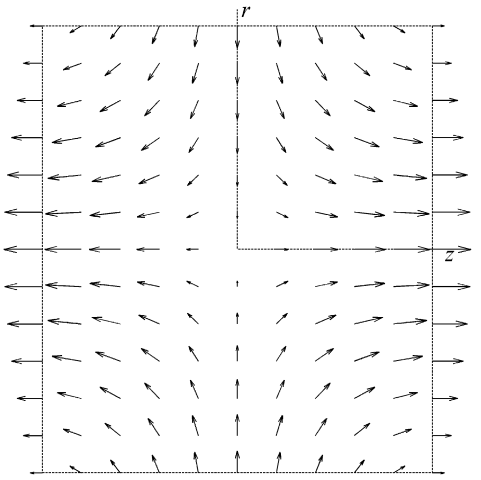

Fig. 2. Mode shape for the symmetric mode $s1$ numerically calculated for an aluminium cylinder with universal slenderness $L/D = 0.853145$ and Poisson's ratio $\nu = 0.329$.

(3) Fig. 2 represents the numerical results for the amplitudes of vibration at different points on an aluminium cylinder of $\nu = 0.329$ and $L/D = 0.853145$ (first universal slenderness ratio) that is vibrating at the first universal frequency. Note that the displacements are, as expected, neither radial nor longitudinal but oblique. The vector field for the amplitude of the displacements takes the form similar to a set of equilateral hyperbolas, where the motion is purely longitudinal at both cylinder ends. Note also from Fig. 2 that at the ends it seems that $\partial U/\partial z + \partial W/\partial r = 0$. Therefore, according to Eq. (1), the shear component p_{rz} is zero, which agrees with Zemanek's predictions.

4. Experimental study

4.1. Experimental arrangement

The cylindrical sample is positioned horizontally and supported at its centre on a small soft rubber block. Longitudinal oscillations are induced by applying an axial impact to the centre of one of the cylinder ends. After the application of the impact, no significant forces act on the sample and the cylinder vibrates almost freely in its natural frequencies. The out-of-plane component of the displacement is detected by means of a laser speckle interferometer OP-35 I/O [21]. Detection is carried out at the central point of the end opposite to that where the impact is applied. The peaks in the spectrum are associated with the natural frequencies for the vibration of the sample.

In a second experiment, two small transducers are glued to the sample. Each one is adhered to an end of the cylinder and they are connected in parallel to a sinusoidal signal generator [22]. Forced vibration is induced by an exciting frequency close to the resonance one. The amplitude and phase of the out-of-plane and in-plane displacement at points along a parallel line to the cylinder axis permit the determination of the mode shapes at the line. The two components of the displacement are measured by the aforementioned I/O laser interferometer.

4.2. Some experimental results

The results of two experiments are described in this section. Other experiments are reported in Section 6.

(1) An experiment with a stainless-steel cylinder of diameter $D = 49.90$ mm and universal slenderness ratio $L/D = 0.85$ yields a value of $\Omega = 2.61$. This result differs from the analytical result by less than 0.4%.

(2) In a new experiment, the mode shape of an aluminium cylinder of $L/D = 0.8531$ and $D = 39.00$ mm vibrating at the first universal point is determined, according to the procedure described in Section 4.1 for forced excitation. The two piezoelectric transducers are connected to the sinusoidal signal generator in order to excite the first symmetric mode. The resonant frequency obtained is 66 710 Hz, i.e. 0.8% smaller than that measured for the free vibration (67 275 Hz), due to the transducer mass added. When detecting the mode shape, the sample is excited by a harmonic force with a frequency of 66 800 Hz, close to the resonant frequency but not equal, since in resonant conditions small variations in the frequency due to the instability of the system cause sharp changes in the response obtained. The aforementioned laser speckle interferometer is used to detect the displacement components at nine points along the cylinder, both in the out-of-plane direction, (Fig. 3), and in the in-plane direction (Fig. 4). The sample is 33.27 mm long and the points are spaced approximately 5 mm apart. The points 1 and 9 are at a distance of 1.54 and 1.24 mm, respectively, from each end. These graphs show that all out-of-plane components have the same phase, the amplitude being a maximum at the central point, while the in-plane component is zero at the centre, maximum at the ends, and the phase is opposite in the two halves of the cylinder. Fig. 5 shows the amplitude of vibration for both components in terms of the position of each point. In such a figure it is observed that for the in-plane component the plot approximately corresponds to half a period of the cosine

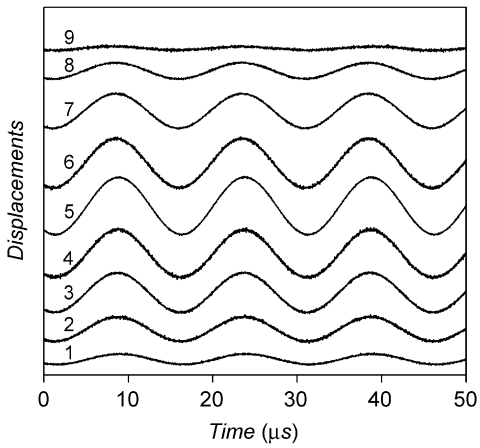

Fig. 3. Experimental results for the out-of-plane displacement components in terms of time, detected at nine points along a straight line on the lateral surface of an aluminium cylinder with a slenderness $L/D = 0.85$.

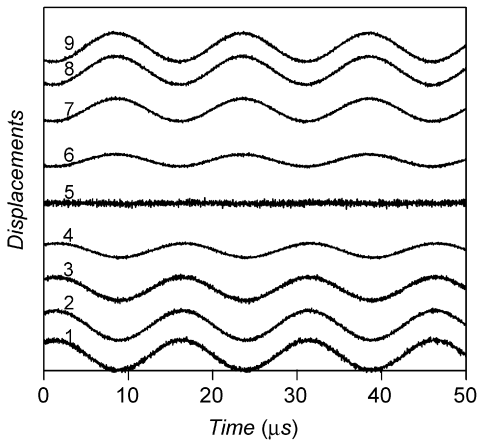

Fig. 4. Same as Fig. 3 for the in-plane displacement component.

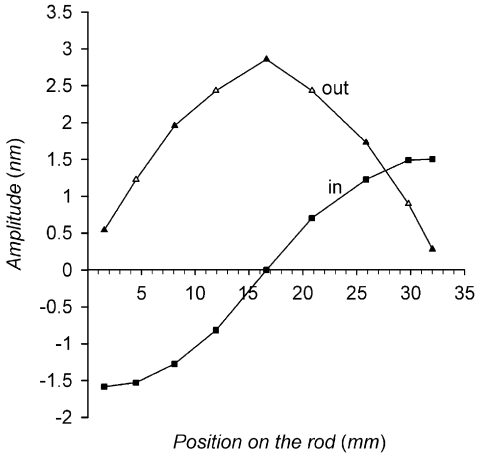

Fig. 5. Amplitudes of the out-of-plane and in-plane components in terms of the position of the nine points.

function, which is in agreement with Zemanek's conclusion [2], which states that at the universal point, a finite-length rod must be an integer number of half-wavelength long. From Fig. 5 it is possible to depict a new figure, not displayed here, showing by arrows the amplitude of vibration of the points of the cylinder along a straight line parallel to its axis. Comparison of the amplitudes from the experimental values with those numerically obtained, shown at the bottom of Fig. 2, shows the good agreement achieved.

5. Analysis of the frequency crossings for cylinders with Poisson's ratio equal to zero

According to the elemental theory for slender bars, the graph showing the non-dimensional frequency as a function of the slenderness for the symmetric and antisymmetric longitudinal modes is a set of non-intersecting hyperbolas. In this theory, there are neither crossings between the symmetric modes themselves, nor between the antisymmetric modes, nor between the symmetric and antisymmetric modes. As there are no two modes with the same frequency, it can be said that there are no multiple frequencies. For short cylinders, the Ω versus L/D curves are complicated; it is, therefore, expected that there is a possibility of finding multiple frequencies.

Crossings between symmetric or antisymmetric axisymmetric modes of cylinders with Poisson's ratio equal to zero are first analysed. As mentioned earlier, the analytical calculation of the axisymmetric natural frequencies of a short cylinder yields some solutions for an ideal material whose Poisson's ratio is zero.

(1) Numerical calculation for the symmetric modes gives the curves of Fig. 1. The detailed numerical study performed leads us to the conclusion that the curves in the Ω–L/D for the three lowest frequencies of the symmetric modes pass through, at least, the point corresponding to the lowest universal slenderness ratio and the lowest universal frequency. As a proof, Fig. 6 shows the three symmetric mode shapes corresponding to the three points on the aforementioned three curves and located on the left-hand side of the first universal point and close to it. Fig. 6a belongs to the straight line of Fig. 1, radial mode, and it corresponds to the lowest frequency, Fig. 6c to the hyperbolic line, longitudinal mode and third frequency, and Fig. 6b to the second mode, vortex mode. If the three symmetric mode shapes on the right-hand side of the first universal point are drawn, the resulting figure will be the same as Fig. 6, but Fig. 6a, corresponding to the radial mode, will be placed at the top (third frequency) whereas Fig. 6c, longitudinal mode and first frequency, at the bottom. Therefore, the crossing of the three lines corresponding to $s1$, $s2$ and $s3$ exists. Hence, there is a multiple frequency of the third order for such three symmetric modes. At the crossing point are an infinite number of mode shapes is possible, but any of that infinite number is merely linear combinations of the three modes shown in Fig. 6. There are other crossing points in Fig. 1.

(2) In the figure for the antisymmetric modes, analogue to Fig. 1 for symmetric modes but not shown here, the curve for the lowest antisymmetric mode $a1$ and that for the higher frequency $a2$ appears to intersect.

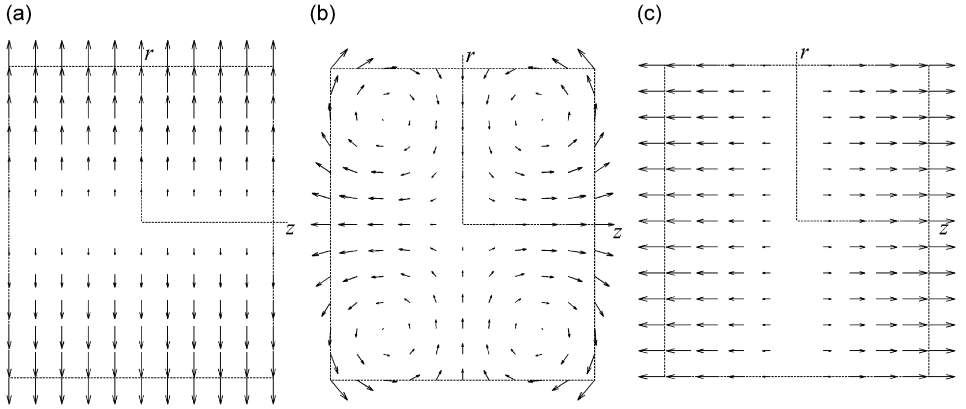

Fig. 6. Mode shapes for $v = 0$ at three points below and close to the universal slenderness: *a* radial, *b* vortex, and *c* longitudinal modes, respectively.

A detailed calculation shows that such a crossing occurs for $L/D = 1.844$, the corresponding frequency being $\Omega = 2.412$. The mode shapes below and above the crossing are interchanged; however they are not shown here. New calculations yield other crossing points in this plot, for instance there is a multiple frequency corresponding to $a2$ and $a3$ for $L/D \approx 1.7$.

A conclusion of the above study is that for Poisson's ratio equal to zero there are many crossings in the graphs of Ω versus L/D and, therefore, multiple frequencies occur in the plot for the symmetric vibrations as well as in that for the antisymmetric vibrations.

6. Analysis of the frequency crossings for cylinders with Poisson's ratio other than zero

Let us now study if multiple frequencies occur in cylinders with a Poisson's ratio other than zero.

(1) A study of the crossing between the two lowest axisymmetric vibration modes of a short cylinder was carried out by the authors [22]. Numerical calculation and experimental tests show that the frequencies of the first symmetric mode, $s1$, and the first antisymmetric mode, $a1$, take the same value for a slenderness $L/D = 0.786$ for a stainless-steel sample.

(2) One of the conclusions of Hutchinson's work [4] is that there are no frequency crossings in any of the plots of the frequency versus slenderness, and that no frequency crossings occur when the plotting is carried out for a given v for even and odd modes separately. This statement seems to contradict the previous analytical and numerical results for materials with a Poisson's ratio of zero. In order to confirm such a statement, the Ritz method described in Section 3 is applied to study the vibration of a stainless-steel cylinder whose Poisson's ratio is 0.298. The results found are shown in Fig. 7 for the symmetric modes. In this figure no crossing is observed at the first universal point, whereas for a Poisson's ratio of zero there is some crossing. A detailed numerical study is carried out in order to determine the apparent crossing between the second and third curves for the symmetric modes, the results show that such a crossing does not occur. Fig. 8 shows the results for the antisymmetric modes. This figure seems to lead to the deduction that the lowest curve would intersect with the following higher curve, if they varied smoothly. The numerical study performed in order to study this apparent crossing in detail has proved that no frequency crossing occurs, which is in agreement with Hutchinson's results. At the apparent crossing for $L/D \approx 1.35$, it is found that $\Omega_{a1} = 2.92$ and $\Omega_{a2} = 3.05$.

The apparent paradox that if Poisson's ratio is zero there are many crossings, while if it is other than zero no crossings occur, is verified by performing new numerical calculations for a material such as glass with a Poisson's ratio as small as 0.217. The results are plotted in Fig. 9, where the curves for both the symmetric and antisymmetric modes are shown; from this figure it is deduced that these curves do not intersect either.

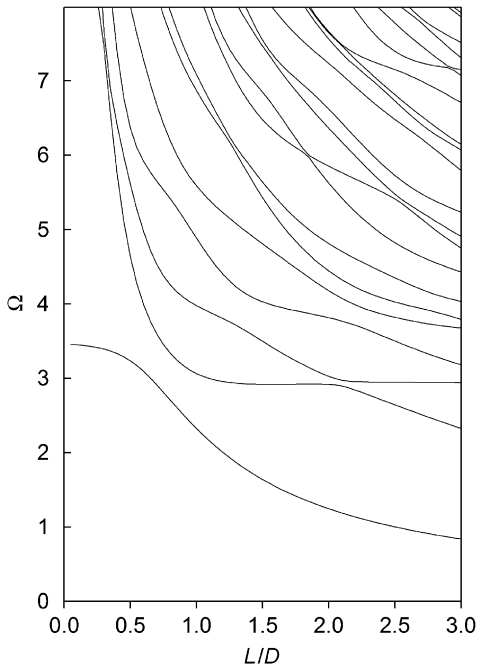

Fig. 7. $\Omega - L/D$ curves for the symmetric modes of a steel cylinder with Poisson's ratio $\nu = 0.298$. It appears that the modes $s2$ and $s3$ cross.

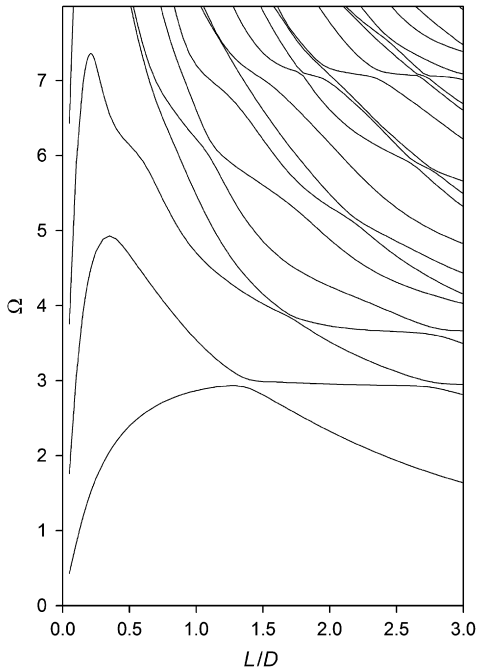

Fig. 8. $\Omega - L/D$ curves for the antisymmetric modes of the steel cylinder. It appears that the modes $a1$ and $a2$ cross in the surroundings of $L/D = 1.3$.

In order to verify such a result and analyse the apparent crossing at approximately $L/D = 1.5$ and $\Omega = 2.8$, a thorough calculation of the non-dimensional frequencies is carried out for the 21 values of the slenderness 1.40, 1.41, …, 1.59, 1.60, which verifies that the difference between frequencies Ω_{a2} and Ω_{a1} can be accurately observed. However, a lot of crosses occur between symmetric and antisymmetric curves.

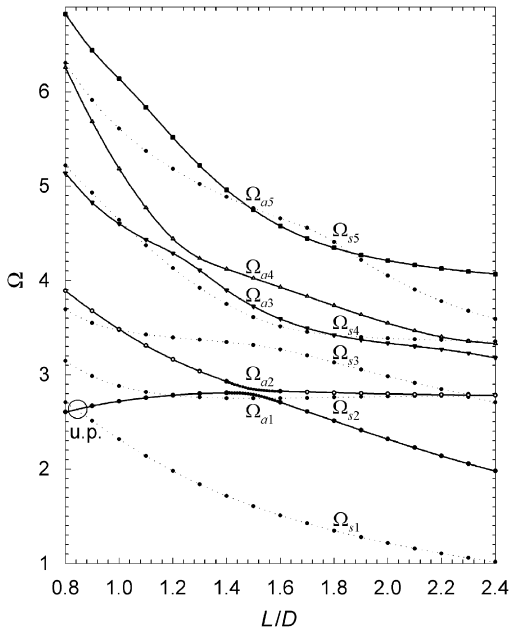

Fig. 9. $\Omega - L/D$ curves for a glass cylinder with $\nu = 0.217$. It appears that the modes $a1$ and $a2$ cross at $L/D = 1.5$.

(3) The mode shapes for stainless-steel cylinders in the neighbourhood of an apparent crossing are also numerically calculated by means of the Ritz method. The study is focussed on the apparent crossing in Fig. 8 at $L/D \approx 1.35$; the cylinders included have slendernesses from 1.2 to 1.6. It is found that as the value of the slenderness L/D increases from a value slightly smaller than that corresponding to the apparent crossing (no crossing actually occurs), the shapes of the two modes gradually tend to become similar. The mode shape for $a1$ below the apparent crossing bears some resemblance to that for $a2$ above such a crossing. Analogously, the mode shapes for $a1$ and that for $a2$ above and below the crossing point, respectively, are similar, i.e. after the apparent crossing, the form of the mode shape seems to be interchanged as is observed in the case of $\nu = 0$.

(4) These results are experimentally verified by determining the natural frequencies and the mode shapes $a1$ and $a2$ for two steel cylinders according to the procedures given in Section 4.1. The steel cylinders have a diameter of 49.00 mm and slendernesses $L/D = 1.2$ and 1.5, below and above the apparent crossing, respectively. Natural frequencies are first obtained. These experimental results are in agreement with those obtained from Figs. 7 and 8. Forced vibration is induced in order to measure the radial and axial components along a straight line on the surface of each cylinder, as described in Section 4.2. The out-of-plane (radial) and in-plane (axial) components of the displacement at points along a straight line of the surface of the cylinder with $L/D = 1.2$ are represented in Fig. 10a and b for the first antisymmetric mode and the second one, respectively. The solid and dashed lines depict the numerical results for the out-of-plane and in-plane components of the displacements along the line. The squares and triangles indicate the amplitudes for the out-of-plane and in-plane components, respectively, measured with the interferometer. Fig. 10c and d shows the results for the cylinder with slenderness $L/D = 1.5$. Note that the experimental results are in complete agreement with the numerical ones. Fig. 10a for the first antisymmetric mode for $L/D = 1.2$ bears some resemblance to Fig. 10d corresponding to the second mode for $L/D = 1.5$. Similarly, Fig. 10b resembles Fig. 10c. Therefore, it is found that although no crossing occurs, the mode shapes gradually tend to become similar, resulting in almost an interchange of the mode shapes.

From the above study it is concluded that for materials with a Poisson's ratio other than zero, no crossing occurs in the curves of Ω versus L/D, neither for the symmetric modes nor for the antisymmetric modes; both statements are limited by the accuracy of the numerical calculations. The plots of the non-dimensional frequencies versus

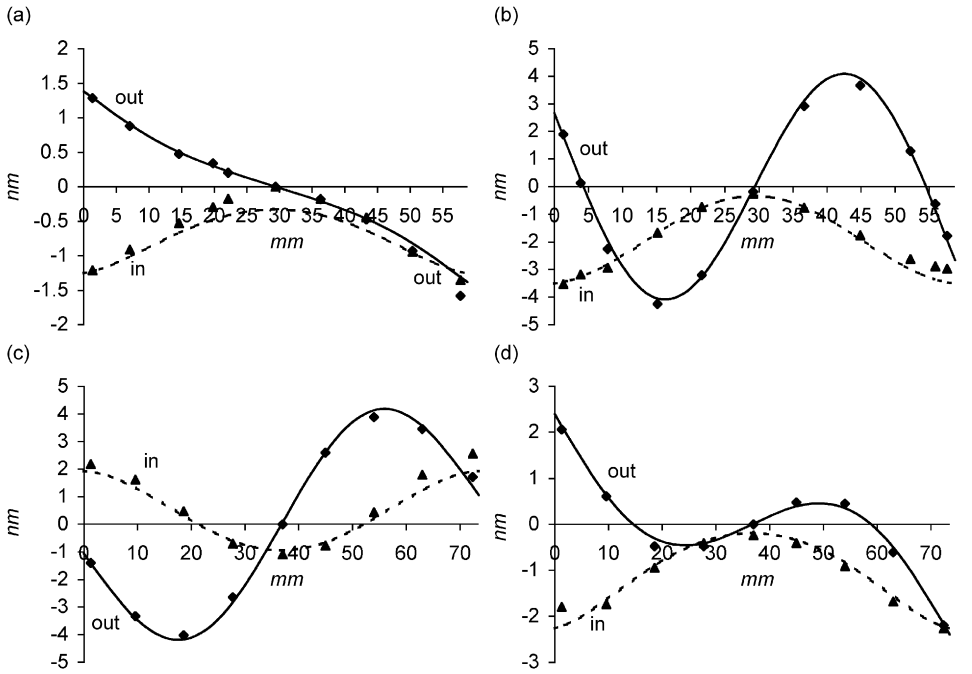

Fig. 10. The out-of-plane and in-plane displacements along a straight line of the surface of a cylinder with $L/D = 1.2$ vibrating in the two lowest antisymmetric modes: (a) for $a1$ and (b) for $a2$. The same for a cylinder with $L/D = 1.5$: (c) for $a1$ and (d) for $a2$.

slenderness show that some curves tend to approach one another closely and then "veer" away. In the veering regions, the minimum difference between the values of the frequencies increases with Poisson's ratio. Similar results have been observed [23] in plotting the variation of frequencies with a system parameter when coupling of the modes exits. On the other hand, for a Poisson's ratio equal to zero, there are many crossings. The vanishing coupling makes it possible to find crossing points for some values of the slenderness.

7. Conclusions

Analytical calculations show that:

(a) Pure radial and longitudinal axisymmetric modes in finite cylinders can occur only if Poisson's ratio is zero, which makes it possible to calculate accurate values of non-dimensional universal frequencies for symmetric modes of vibration of a cylinder.
(b) The existence of a multiple frequency is proved for symmetric modes if $\nu = 0$, the analysis yields accurate value of universal aspect ratio.

The Ritz method leads to:

(c) Possible frequency crossing points are accurately analysed by applying an optimized new procedure that assures the desired degree of convergence.
(d) It is concluded that when curves $\Omega - L/D$ are plotted separately for symmetric and antisymmetric modes there are no frequency crossings, neither between antisymmetric modes nor between symmetric ones, unless Poisson's ratio is null.

The laboratory experiments prove that:

(e) Measurement of the mode shape of a cylinder with the first universal slenderness ratio using a speckle interferometry technique agrees with the numerical predictions that at resonance the value of half-wavelength is the same as the length of the cylinder.
(f) Numerical and experimental results show that a certain similarity between the mode shapes above and below the apparent crossing point exists as if an interchange had taken place.

Acknowledgement

This work has been partially supported by the Spanish Governmental *Plan Nacional de I+D+i 2004-2007* under Project No. BIA2004-07428-C02 of the *Programa Nacional de Construcción*.

References

[1] T.R. Meeker, A.H. Meitzler, *Physical Acoustics*, Vol. 1A, Academic, New York, 1964, pp. 111–167.
[2] J. Zemanek, An experimental and theoretical investigation of elastic wave propagation in a cylinder, *Journal of the Acoustical Society of America* 51 (1972) 265–283.
[3] L. Kari, Axially symmetric modes in finite cylinders—the wave guide solution, *Wave Motion* 37 (2003) 191–206.
[4] J.R. Hutchinson, Vibrations of solid cylinders, *Journal of Applied Mechanics* 47 (1980) 901–907.
[5] J.R. Hutchinson, Vibrations of solid cylinders revisited, *Journal of Applied Mechanics* 62 (1995) 818–819.
[6] J.R. Hutchinson, Axisymmetric vibrations of a free finite-length rod, *Journal of the Acoustical Society of America* 51 (1972) 233–240.
[7] J.R. Hutchinson, Axisymmetric flexural vibrations of a thick free circular plate, *Journal of Applied Mechanics* 46 (1979) 139–144.
[8] J.R. Hutchinson, Comments on "Accurate vibration frequencies of circular cylinders from three-dimensional analysis," *Journal of the Acoustical Society of America* 100 (1996) 1894–1895.
[9] J.R. Hutchinson, Comments on "Comparisons of vibration frequencies for rods and beams from one-dimensional and three-dimensional analysis," *Journal of the Acoustical Society of America* 100 (1996) 1890–1892.
[10] C.P. Lusher, W.N. Hardy, Axisymmetric free vibrations of a transversely isotropic finite cylindrical rod, *Journal of Applied Mechanics* 55 (1988) 855–862.
[11] M. Rumerman, S. Raynor, Natural frequencies of finite circular cylinders in axially symmetric longitudinal vibration, *Journal of Sound and Vibration* 15 (1971) 529–543.
[12] M. Senoo, T. Mishimura, Measurement of elastic constants of polycrystals by the resonance method in a cylindrical specimen, *Bulletin of JSME* 27 (1984) 2339–2346.
[13] P.R. Heyliger, Axisymmetric free vibrations of finite anisotropic cylinders, *Journal of Sound and Vibration* 148 (1991) 507–520.
[14] W.M. Visscher, A. Migliori, T.M. Bell, R.A. Reinert, On the normal modes of free vibration of inhomogeneous and anisotropic elastic objects, *Journal of the Acoustical Society of America* 90 (1991) 2154–2162.
[15] P.R. Heyliger, A. Jilani, The free vibrations of inhomogeneous elastic cylinders and spheres, *International Journal of Solids and Structures* 29 (1992) 2689–2708.
[16] P.R. Heyliger, W.L. Johnson, Traction-free vibration of finite trigonal elastic cylinders, *Journal of the Acoustical Society of America* 113 (2003) 1812–1825.
[17] A.W. Leissa, J. So, Comparisons of vibration frequencies for rods and beams from one-dimensional and three-dimensional analyses, *Journal of the Acoustical Society of America* 98 (1995) 2122–2135.
[18] F.J. Nieves, A. Bayón, F. Gascón, Optimization of the Ritz method to calculate axisymmetric natural vibration frequencies of cylinders, *Journal of Sound and Vibration* in press, available online 5 November 2007, doi:10.1016/j.jsv.2007.09.010.
[19] C.R.C., *Standard Mathematical Tables*, The Chemical Rubber Co., Cleveland, 1964, p. 463.
[20] F.J. Nieves, F. Gascón, A. Bayón, On the natural frequencies of short cylinders and the universal point. Direct determination of the shear modulus, *Journal of the Acoustical Society of America* 115 (2004) 2928–2936.
[21] J.P. Monchalin, J.D. Aussel, R. Heon, C.K. Jen, A. Boundreault, R. Bernier, Measurements of in-plane and out-of-plane ultrasonic displacements by optical heterodyne interferometry, *Journal of Nondestructive Evaluation* 8 (1989) 121–132.
[22] F.J. Nieves, F. Gascón, A. Bayón, A multiple frequency in the two lowest axisymmetric vibration modes of a short cylinder, *Journal of Sound and Vibration* 251 (2002) 741–749.
[23] N.C. Perkins, C.D. Mote, Comments on curve veering in eigenvalue problems, *Journal of Sound and Vibration* 106 (1986) 451–463.